Designation: E598 – 08 (Reapproved 2020)

Standard Test Method for Measuring Extreme Heat-Transfer Rates from High-Energy Environments Using a Transient, Null-Point Calorimeter[1]

This standard is issued under the fixed designation E598; the number immediately following the designation indicates the year of original adoption or, in the case of revision, the year of last revision. A number in parentheses indicates the year of last reapproval. A superscript epsilon (ε) indicates an editorial change since the last revision or reapproval.

1. Scope

1.1 This test method covers the measurement of the heat-transfer rate or the heat flux to the surface of a solid body (test sample) using the measured transient temperature rise of a thermocouple located at the null point of a calorimeter that is installed in the body and is configured to simulate a semi-infinite solid. By definition the null point is a unique position on the axial centerline of a disturbed body which experiences the same transient temperature history as that on the surface of a solid body in the absence of the physical disturbance (hole) for the same heat-flux input.

1.2 Null-point calorimeters have been used to measure high convective or radiant heat-transfer rates to bodies immersed in both flowing and static environments of air, nitrogen, carbon dioxide, helium, hydrogen, and mixtures of these and other gases. Flow velocities have ranged from zero (static) through subsonic to hypersonic, total flow enthalpies from 1.16 to greater than 4.65×10^1 MJ/kg (5×10^2 to greater than 2×10^4 Btu/lb.), and body pressures from 10^5 to greater than 1.5×10^7 Pa (atmospheric to greater than 1.5×10^2 atm). Measured heat-transfer rates have ranged from 5.68 to 2.84×10^2 MW/m^2 (5×10^2 to 2.5×10^4 Btu/ft^2-sec).

1.3 The most common use of null-point calorimeters is to measure heat-transfer rates at the stagnation point of a solid body that is immersed in a high pressure, high enthalpy flowing gas stream, with the body axis usually oriented parallel to the flow axis (zero angle-of-attack). Use of null-point calorimeters at off-stagnation point locations and for angle-of-attack testing may pose special problems of calorimeter design and data interpretation.

1.4 *This standard does not purport to address all of the safety concerns, if any, associated with its use. It is the responsibility of the user of this standard to establish appropriate safety, health, and environmental practices and determine the applicability of regulatory limitations prior to use.*

1.5 *This international standard was developed in accordance with internationally recognized principles on standardization established in the Decision on Principles for the Development of International Standards, Guides and Recommendations issued by the World Trade Organization Technical Barriers to Trade (TBT) Committee.*

2. Referenced Documents

2.1 *ASTM Standards:*[2]

E422 Test Method for Measuring Heat Flux Using a Water-Cooled Calorimeter

E511 Test Method for Measuring Heat Flux Using a Copper-Constantan Circular Foil, Heat-Flux Transducer

3. Terminology

3.1 *Symbols:*

a = Radius of null-point cavity, m (in.)
b = Distance from front surface of null-point calorimeter to the null-point cavity, m (in.)
C_p = Specific heat capacity, J/kg–K (Btu/lb-°F)
d = Diameter of null-point cavity, m (in.)
k = Thermal conductivity, W/m–K (Btu/in.-sec-°F)
L = Length of null-point calorimeter, m (in.)
q = Calculated or measured heat flux or heat-transfer-rate, W/m^2 (Btu/ft^2-sec)
q_0 = Constant heat flux or heat-transfer-rate, W/m^2 (Btu/ft^2-sec)
R = Radial distance from axial centerline of TRAX analytical model, m (in.)
r = Radial distance from axial centerline of null-point cavity, m (in.)
T = Temperature, K (°F)
T_b = Temperature on axial centerline of null point, K (°F)
T_s = Temperature on surface of null-point calorimeter, K (°F)
t = Time, sec
Z = Distance in axial direction of TRAX analytical model, m (in.)

[1] This test method is under the jurisdiction of ASTM Committee E21 on Space Simulation and Applications of Space Technology and is the direct responsibility of Subcommittee E21.08 on Thermal Protection.

Current edition approved Nov. 1, 2020. Published December 2020. Originally approved in 1977. Last previous edition approved in 2015 as E598 – 08(2015). DOI: 10.1520/E0598-08R20.

[2] For referenced ASTM standards, visit the ASTM website, www.astm.org, or contact ASTM Customer Service at service@astm.org. For *Annual Book of ASTM Standards* volume information, refer to the standard's Document Summary page on the ASTM website.

α = Thermal diffusivity, m^2/sec ($in.^2$/sec)
ρ = Density, kg/m^3 ($lb/in.^3$)

4. History of Test Method

4.1 From literature reviews it appears that Masters and Stein (**1**)[3] were the first to document the results of an analytical study of the temperature effects of axial cavities drilled from the backside of a wall which is heated on the front surface (see Fig. 1). These investigators were primarily concerned with the deviation of the temperature measured in the bottom of the cavity from the undisturbed temperature on the heated surface. Since they were not in possession of either the computing power or the numerical heat conduction codes now available to the analyst, Masters and Stein performed a rigorous mathematical treatment of the deviation of the transient temperature, T_b, on the bottom centerline of the cavity of radius, a, and thickness, b, from the surface temperature T_s. The results of Masters and Stein indicated that the error in temperature measurement on the bottom centerline of the cavity would decrease with increasing values of a/b and also decrease with increasing values of the dimensionless time, $\alpha t/b^2$, where α is the thermal diffusity of the wall material. They also concluded that the most important factor in the error in temperature measurement was the ratio a/b and the error was independent of the level of heat flux. The conclusions of Masters and Stein may appear to be somewhat elementary compared with our knowledge of the null-point concept today. However, the identification and documentation of the measurement concept was a major step in leading others to adapt this concept to the transient measurement of high heat fluxes in ground test facilities.

4.2 Beck and Hurwicz (**2**) expanded the analysis of Masters and Stein to include steady-state solutions and were the first to label the method of measurement "the null-point concept." They effectively used a digital computer to generate relatively large quantities of analytical data from numerical methods. Beck and Hurwicz computed errors due to relatively large thermocouple wires in the axial cavity and were able to suggest that the optimum placement of the thermocouple in the cavity occurred when the ratio a/b was equal to 1.1. However, their analysis like that of Masters and Stein was only concerned with the deviation of the temperature in the axial cavity and did not address the error in measured heat flux.

4.3 Howey and DiCristina (**3**) were the first to perform an actual thermal analysis of this measurement concept. Although the explanation of modeling techniques is somewhat ambiguous in their paper, it is obvious that they used a finite element, two dimensional axisymmetric model to produce temperature profiles in a geometry simulating the null-point calorimeter. Temperature histories at time intervals down to 0.010 sec were obtained for a high heat-flux level on the surface of the analytical model. Although the analytical results are not presented in a format which would help the user/designer optimize the sensor design, the authors did make significant general conclusions about null point calorimeters. These include: (*1*) "..., thermocouple outputs can yield deceivingly fast

[3] The boldface numbers in parentheses refer to the list of references at the end of this test method.

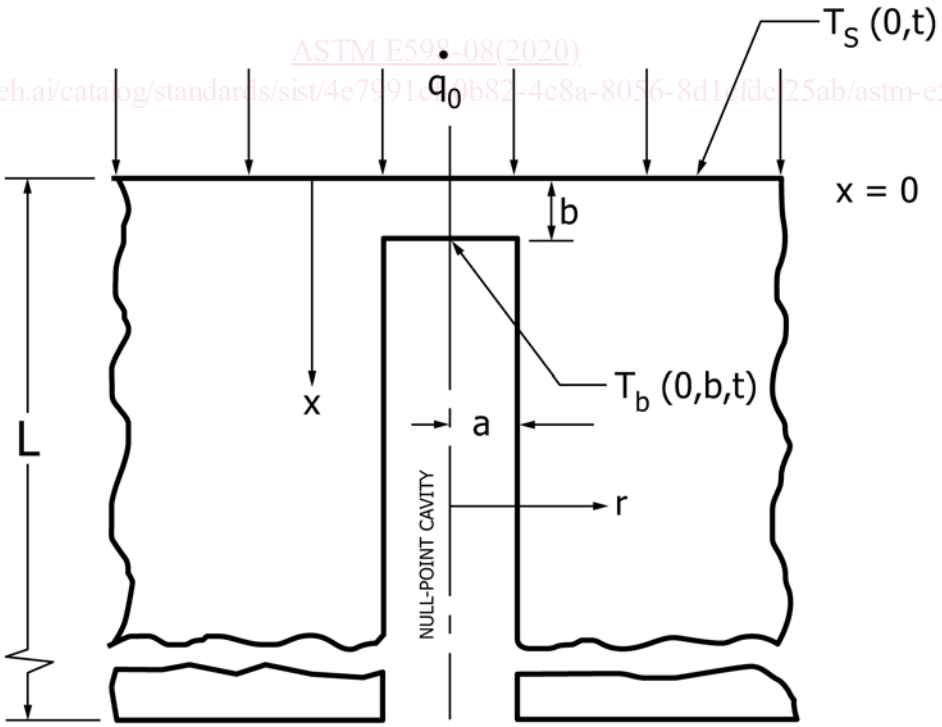

NOTE 1—1-T_s(0,t) = Surface temperature (x = 0) of a solid, semi-infinite slab at some time, t.
NOTE 2—2-T_b(0,b,t) = Temperature at r = 0, x = b of a slab with a cylindrical cavity at some time, t, heat flux, q, the same in both cases.

FIG. 1 Semi-infinite Slab with Cylindrical Cavity

response rates and erroneously high heating rates (+ 18 %) when misused in inverse one-dimensional conduction solutions." (*2*) "The prime reason for holding the thermocouple depth at $R/E = 1.1$ is to maximize thermocouple response at high heating rates for the minimum cavity depth..." (Note: *R* and *E*as used by Howey and DeChristina are the same terms as *a* and *b* which are defined in 4.1 and are used throughout this document.) (*3*) A finite length null-point calorimeter body may be considered semi-infinite for:

$$\frac{(\alpha t)}{L^2} \leq 0.3$$

4.4 Powars, Kennedy, and Rindal (**4** and **5**) were the first to document using null point calorimeters in the swept mode. This method which is now used in almost all arc facilities has the advantages of (*1*) measuring the radial distributions across the arc jet, and (*2*) preserving the probe/sensor structural integrity for repeated measurements. This technique involves sweeping the probe/sensor through the arc-heated flow field at a rate slow enough to allow the sensor to make accurate measurements, yet fast enough to prevent model ablation.

4.4.1 Following the pattern of Howey and DiCristina, Powars et. al. stressed the importance of performing thermal analyses to "characterize the response of a typical real null point calorimeter to individually assess a variety of potential errors, ...". Powars et. al. complain that Howey & DiCristina "... report substantial errors in some cases, but present no generalized results or design guide lines." They state concerning the analyses performed to support their own documentation, "In order to establish guidelines for null point calorimeter design and data reduction, analyses were performed to individually assess the measurement errors associated with a variety of non-ideal aspects of actual calorimeters." The conclusions reached from the results of the thermal analyses were broken down into eight sub headings and were discussed individually. Some of the conclusions reached were rather elementary and were previously reported in Refs (**1-3**). Others were somewhat arbitrary and were stated without substantiating data. One specific conclusion concerns the ratio of the null-point cavity radius, *a*, to the cavity thickness, *b*. While stating that the optimum condition occurred when $a = b$, the authors of Ref (**4**)further state that when $a = 0.305$ mm (0.012 in.) and $b = 0.127$ mm (0.005 in.); $a/b = 2.4$, the calculated heat flux will be 20 % higher than the actual heat flux. In more recent documentation using more accurate and sophisticated heat conduction computer codes as well as an established numerical inverse heat conduction equation (**6**), the error in indicated heat flux is shown to be considerably higher than 20 % and is highly time dependent.

4.5 The latest and most comprehensive thermal analysis of the null-point calorimeter concept was performed by Kidd and documented in Refs (**6** and **7**). This analytical work was accomplished by using a finite element axisymmetric heat conduction code (**7**). The finite element model simulating the null-point calorimeter system is comprised of 793 finite elements and 879 nodal points and is shown in block diagram form in Fig. 2. Timewise results of normalized heat flux for different physical dimensional parameters (ratios of *a*to *b*) are graphically illustrated on Figs. 3 and 4. The optimum value of the ratio *a/b* is defined to be that number which yields the fastest time response to a step heat-flux input and maintains a constant value of indicated $\dot{q}$/input $\dot{q}$ after the initial time response period. From Figs. 3 and 4, it can be seen that this optimum value is about 1.4 for two families of curves for which the cavity radius, *a*, is held constant while the cavity thickness, *b*, is varied to span a wide range of the ratio *a/b*. This is a slightly higher value than reported by earlier analysts. It is important to note that the analytical results do not necessarily have to give a value of indicated $\dot{q}$/input $\dot{q} = 1.0$ since this difference can be calibrated in the laboratory. The data graphically illustrated on Figs. 3 and 4 and substantiate conclusions drawn by the authors of Refs (**3** and **4**) that the calculated heat flux can be considerably higher than the actual input heat flux—especially as the ratio of *a/b* is raised consistently above 1.5. All of the users of null-point calorimeters assume that the device simulates a semi-infinite body in the time period of interest. Therefore, the sensor is subject to the finite body length, *L*, defined by $L/(\alpha t)^{1/2} \leq 1.8$ in order that the error in indicated heat flux does not exceed one percent (**6** and **7**). This restriction agrees well with the earlier work of Howey and DiCristina (**3**).

4.6 A section view sketch of a typical null-point calorimeter showing all important components and the physical configuration of the sensor is shown in Fig. 5. The outside diameter is 2.36 mm (0.093 in.), the length is 10.2 mm (0.40 in.), and the body material is oxygen-free high conductivity (OFHC) copper. Temperature at the null point is measured by a 0.508 mm (0.020 in.) diam American National Standards Association (ANSI) type K stainless steel-sheathed thermocouple with 0.102 mm (0.004 in.) diam thermoelements. Although no thermocouple attachment is shown, it is assumed that the individual thermocouple wires are in perfect contact with the backside of the cavity and present no added thermal mass to the system. Details of installing thermocouples in the null point cavity and making a proper attachment of the thermocouple with the copper slug are generally considered to be proprietary by the sensor manufacturers. Kidd in Ref (**7**) states that the attachment is made by thermal fusion without the addition of foreign materials. Note that the null-point body has a small flange at the front and back which creates an effective dead air space along the length of the cylinder to enhance one-dimensional heat conduction and prevent radial conduction. For aerodynamic heat-transfer measurements, the null-point sensors are generally pressed into the stagnation position of a sphere cone model of the same material (OFHC copper).

4.7 The value of the lumped thermal parameter of copper is not a strong function of temperature. In fact, the value of $(\rho C_p k)^{1/2}$ for OFHC copper varies less than three percent from room temperature to the melting point, 1356 K (1981 °F); (see Fig. 6). Thermal properties of OFHC copper are well documented and data from different sources are in good agreement (**8**). Most experimenters use the room temperature value of the parameter in processing data from null-point calorimeters.

4.8 The determination of surface heat flux as a function of time and temperature requires a digital computer, programmed to calculate the correct values of heat-transfer rate. Having the

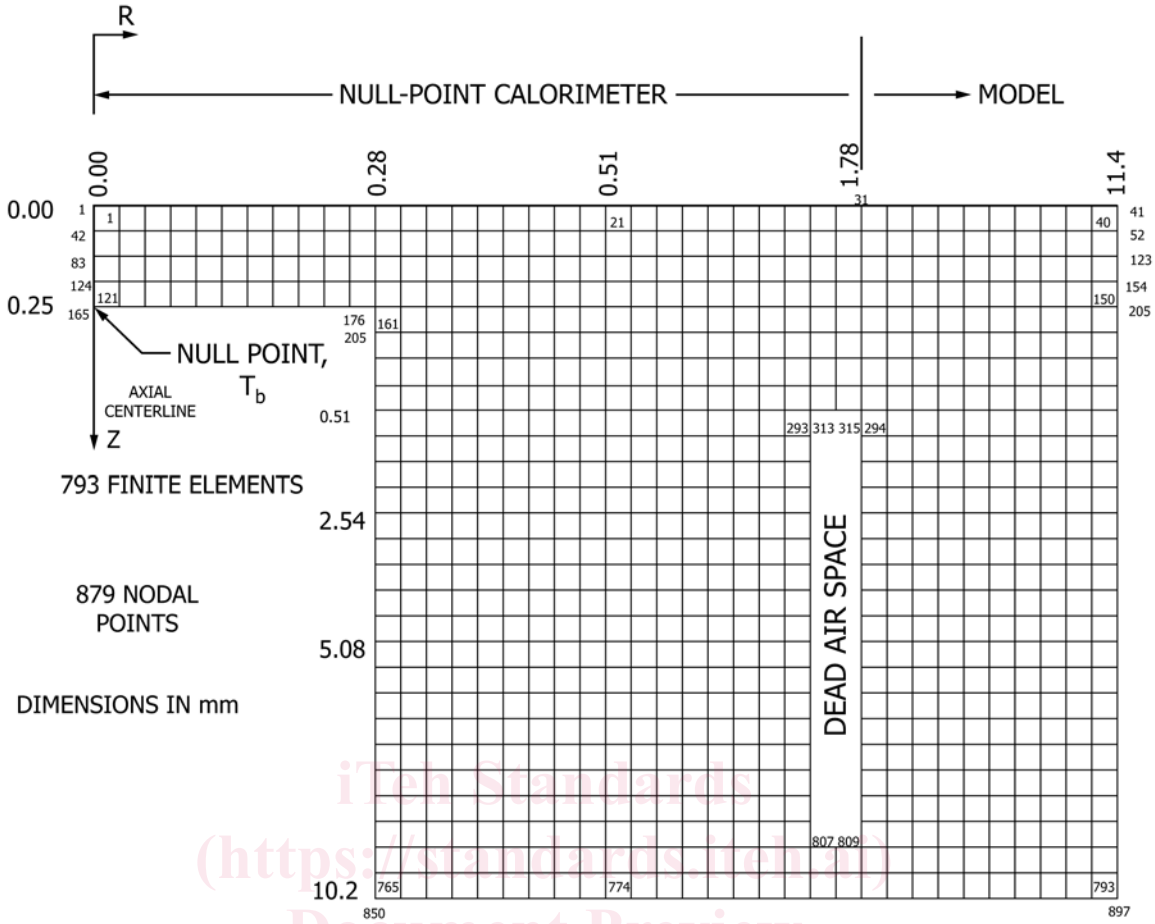

FIG. 2 Finite Element Model of Null-Point Calorimeter

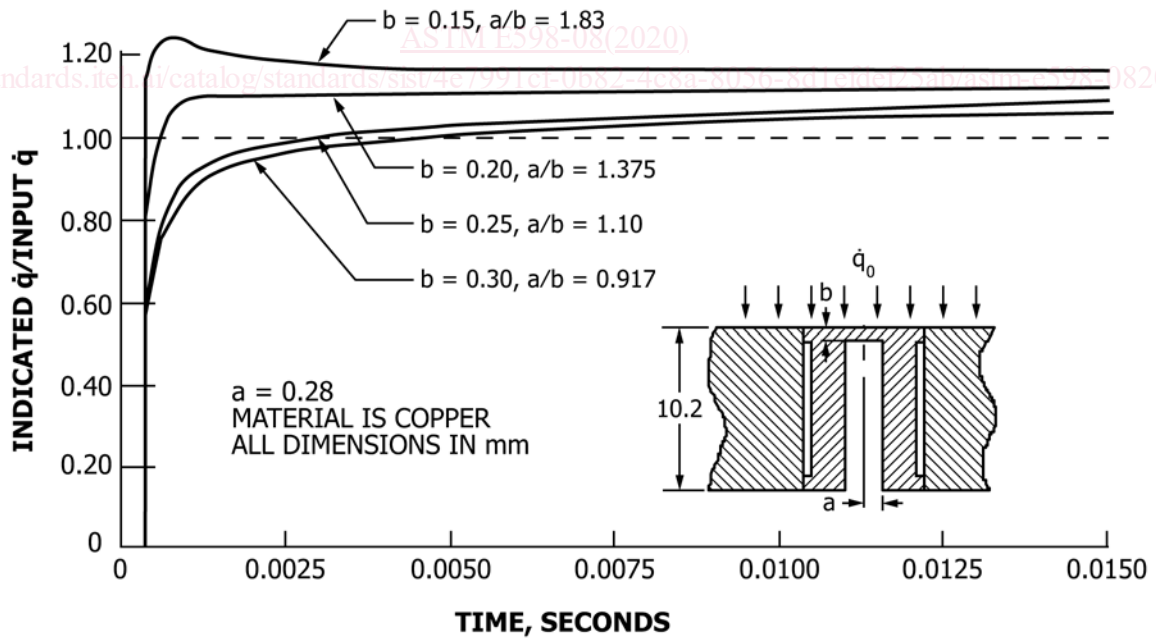

FIG. 3 Null-Point Calorimeter Analytical Time Response Data

measured null-point cavity temperature, the problem to be solved is the inverse problem of heat conduction. Several versions of the well known Cook and Felderman numerical integration equation (**9**) can be used to obtain the surface heat flux as a function of time. These equations are described in Section 10.

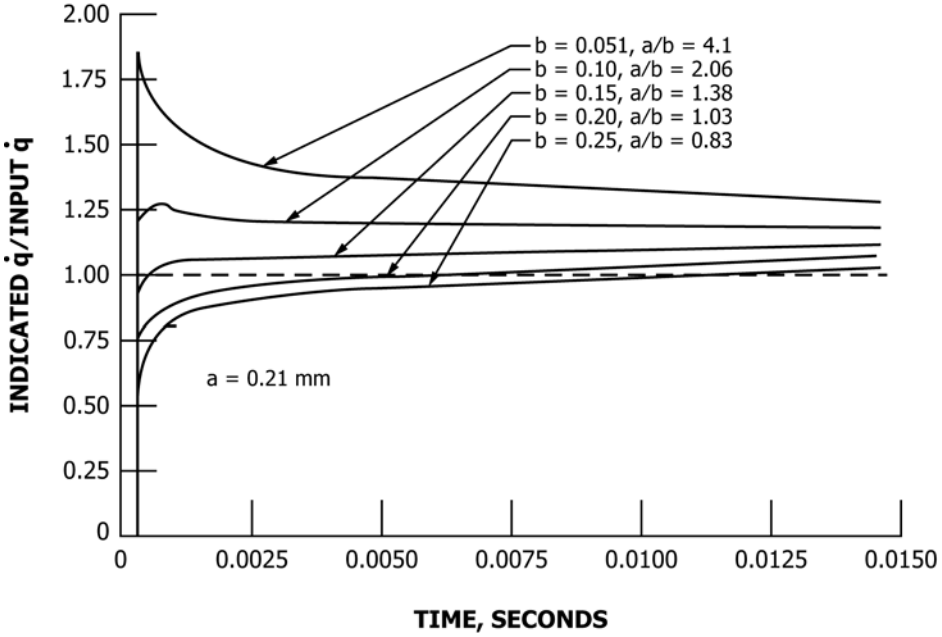

FIG. 4 Null-Point Calorimeter Analytical Time Response Data

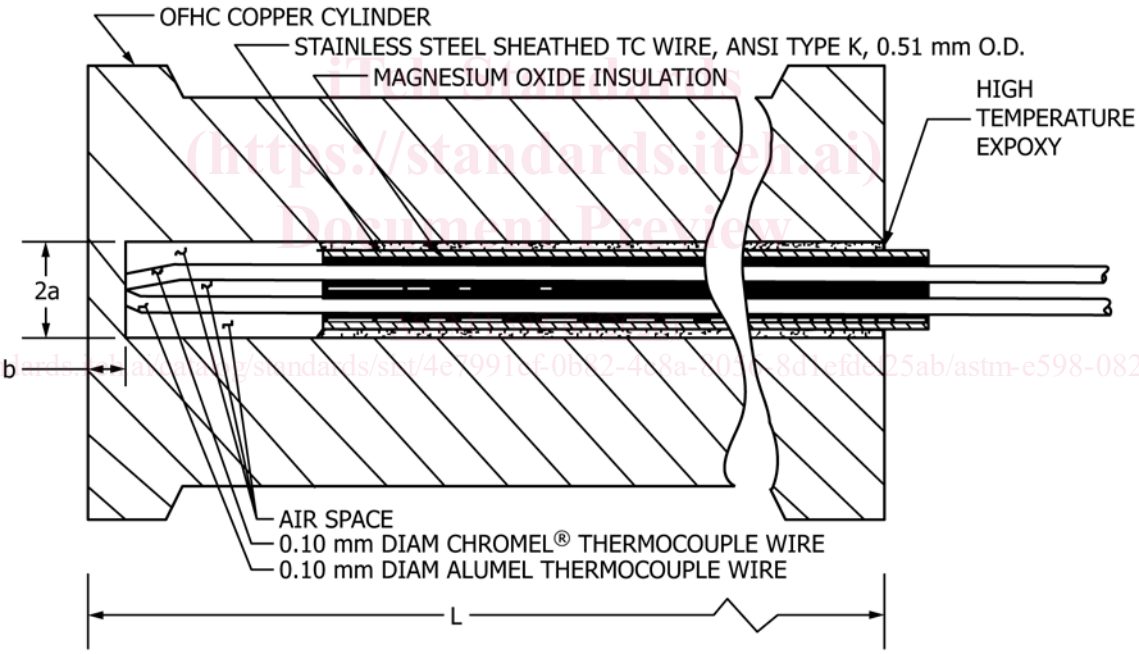

FIG. 5 Section View Sketch of Null-Point Calorimeter

5. Significance and Use

5.1 The purpose of this test method is to measure extremely high heat-transfer rates to a body immersed in either a static environment or in a high velocity fluid stream. This is usually accomplished while preserving the structural integrity of the measurement device for multiple exposures during the measurement period. Heat-transfer rates ranging up to 2.84×10^2 MW/m^2 (2.5×10^4 Btu/ft^2-sec) (**7**) have been measured using null-point calorimeters. Use of copper null-point calorimeters provides a measuring system with good response time and maximum run time to sensor burnout (or ablation). Null-point calorimeters are normally made with sensor body diameters of 2.36 mm (0.093 in.) press-fitted into the nose of an axisymmetric model.

5.2 Sources of error involving the null-point calorimeter in high heat-flux measurement applications are extensively discussed in Refs (**3-7**). In particular, it has been shown both analytically and experimentally that the thickness of the copper above the null-point cavity is critical. If the thickness is too great, the time response of the instrument will not be fast enough to pick up important flow characteristics. On the other hand, if the thickness is too small, the null-point calorimeter

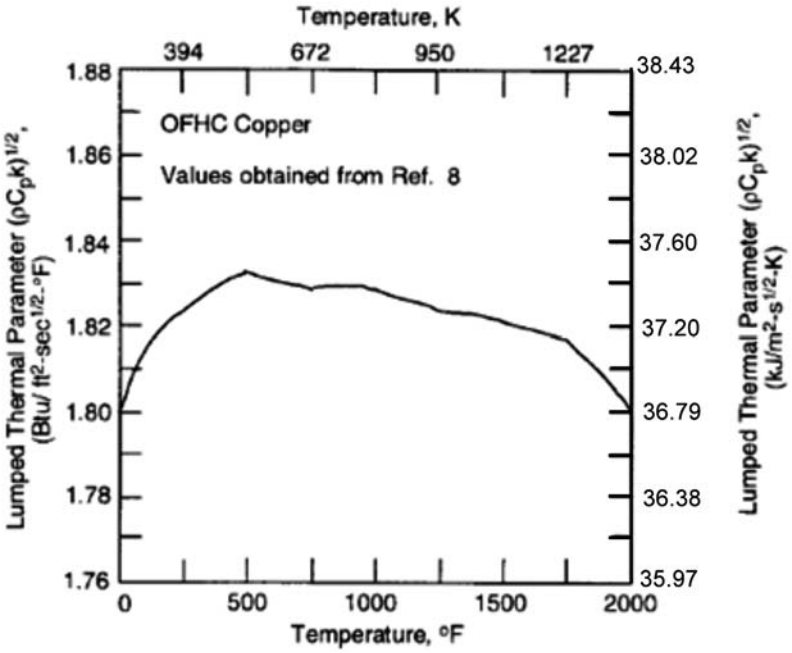

FIG. 6 Variation of $(\rho C_p k)^{1/2}$ with Temperature

will indicate significantly larger (and time dependent) values than the input or incident heat flux. Therefore, all null-point calorimeters should be experimentally checked for proper time response and calibration before they are used. Although a calibration apparatus is not very difficult or expensive to fabricate, there is only one known system presently in existence (**6** and **7**). The design of null-point calorimeters can be accomplished from the data in this documentation. However, fabrication of these sensors is a difficult task. Since there is not presently a significant market for null-point calorimeters, commercial sources of these sensors are few. Fabrication details are generally regarded as proprietary information. Some users have developed methods to fabricate their own sensors (**7**). It is generally recommended that the customer should request the supplier to provide both transient experimental time response and calibration data with each null-point calorimeter. Otherwise, the end user cannot assume the sensor will give accurate results.

5.3 Interpretation of results from null-point calorimeters will, in general, be the same as for other heat-flux sensors operating on the semi-infinite solid principle such as coaxial surface thermocouples and platinum thin-film gages. That is, the effects of surface chemical reactions, gradients in the local flow and energy fields, thermal radiation, and model alignment relative to the flow field vector will produce the same qualitative results as would be experienced with other types of heat flux sensors. In addition, signal conditioning and data processing can significantly influence the interpretation of null-point calorimeter data.

6. Apparatus

6.1 In general, the null-point sensor shall consist of an OFHC copper hollow thick wall cylinder (closed on one end) with a fine wire thermocouple attached on the axial centerline in the bottom of the null-point cavity. The sensor assembly shall be configured to thermally simulate a semi-infinite solid in the time period of interest. The null-point cylinder will be flanged at the front and back to provide a thermally insulating air gap between the body of the sensor and the copper model as shown in Fig. 7. The sensor is normally installed in the model by press fitting. The null-point cavity radius-to-subsurface depth ratio *a/b*, shall be about (but not greater than) 1.4 (**6** and **7**). The temperature sensor is usually a 0.508 mm (0.020 in.) diam stainless steel sheathed thermocouple wire with Chromel-Alumel (ANSI type K) thermoelements (0.102 mm; [0.004 in.] diam).

6.2 During data acquisition, the null-point calorimeter thermocouple output signal is recorded at a rate which will define the desired facility flow fluxuations. A common data sampling rate is 5000 points/sec with a 1 kHz analog filter. Data are normally recorded on disk file and can be transferred to another data storage medium. The raw analog data are normally smoothed before numerical integration techniques are employed to obtain the processed or reduced heat flux data. Discussions of smoothing techniques and numerical integration methods can be found in Refs (**6** and **7**), respectively.

7. Experimental Time Response

7.1 It was shown by thermal analysis in Figs. 3 and 4 that proper time response was critical for the accurate use of null-point calorimeters in arc facility heat-flux measurement applications. Figs. 3 and 4 show that null point calorimeters can respond too quickly, thus indicating a significantly higher level than the actual heat flux incident upon the instrument's sensing surface. And, of course, null-point sensors can easily be too slow for the intended application. Therefore, the capability of performing experimental time response characterizations at high heat-flux levels in the laboratory is of vital

TYPICAL DIMENSIONS		
	mm	in.
a	0.318	0.0125
b	0.229	0.009
c	0.102	0.004
d	2.03	0.080
D	2.36	0.093
L	10.2	0.400
R_B	6.35	0.250

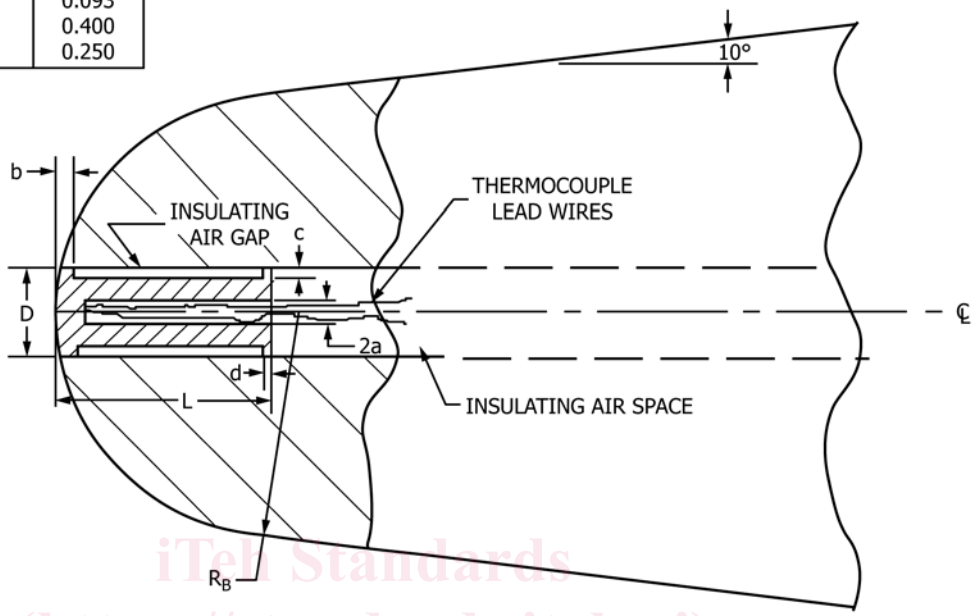

FIG. 7 Typical Null-Point Calorimeter Installation

importance. A prevailing misconception held by many users is that it is not possible to determine the actual time response of null-point sensors in the laboratory. Commercial suppliers of null-point calorimeters are presently unable to supply time response data with their sensors. Methods for obtaining null-point calorimeter experimental time response data have been developed for use at the Arnold Engineering Development Center (AEDC) and are documented in Refs (**6** and **7**). The experimental data generally complement the analytical data, thereby enhancing the credibility of both methods.

7.2 A calibration system which was developed at the AEDC to experimentally determine the time response of null-point calorimeters uses a xenon arc lamp as the heat source and a fast response (5.1 m/sec) [200 in./sec] shuttering device. Fig. 8 shows graphical illustrations of experimental time response data obtained from a null-point sensor. These data were generated by irradiating a single null-point sensor with a high level (19.3 MW/m^2) constant heat flux from the xenon arc lamp very quickly with the fast shutter and recording the timewise output at 0.2-m/sec time intervals. The timewise output was converted to a temperature history by applying the appropriate equations for a type K thermocouple. As shown in Fig. 8, the null-point cavity temperature increased by nearly 97 K (175 °F) in less than 30 m/sec. The resulting timewise heat flux on Fig. 8 was obtained by inserting the temperature history into (Eq 1) and applying the room temperature thermal properties of OFHC copper. A time response of 3 to 4 m/sec to full scale output is indicated by the timewise heat-flux data.

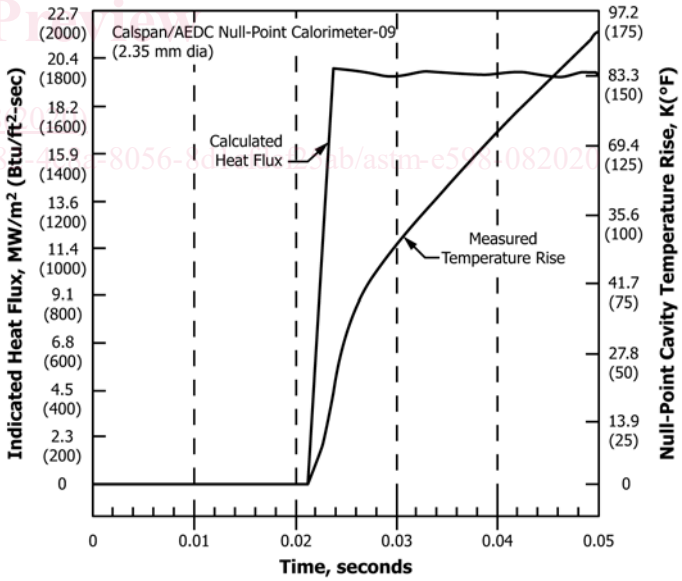

FIG. 8 Null-Point Calorimeter Experimental Time Response Data

These data represent near optimum sensor behavior. If the copper foil thickness above the null-point cavity was thinner, operating behavior such as exhibited by the thin sections on Figs. 3 and 4 probably would have resulted.

8. Calibration

8.1 Thermal analyses of the null-point concept show that small changes in physical dimensions of null-point sensors can